International Journal on Magnetic Particle Imaging
Vol 3, No 2, Article ID 1706006, 5 Pages

Infinite Science Publishing

Research Article

A versatile MPI System Function Viewer

Ulrich Heinen[a,*] · Alexander Weber[b,†] · Jochen Franke[b] · Heinrich Lehr[b] · Olaf Kosch[c]

[a] University of Applied Sciences Pforzheim, Pforzheim, Germany
[b] Bruker BioSpin MRI GmbH, Ettlingen, Germany
[c] Physikalisch-Technische Bundesanstalt, Berlin, Germany
[†] Present address: ITK Engineering AG, Rülzheim, Germany
[*] Corresponding author, email: ulrich.heinen@hs-pforzheim.de

Received 24 November 2016; Accepted 6 March 2017; Published online 22 June 2017

© 2017 Heinen; licensee Infinite Science Publishing GmbH
This is an Open Access article distributed under the terms of the Creative Commons Attribution License (http://creativecommons.org/licenses/by/4.0), which permits unrestricted use, distribution, and reproduction in any medium, provided the original work is properly cited.

Abstract

Magnetic Particle Imaging (MPI) is a versatile new imaging technique for mapping the spatial distribution of magnetic nanoparticle (MNP) based tracers *in vivo* and in real time with high sensitivity. Reconstruction of 3D-encoded MPI data with high temporal resolution so far relies on the so-called system matrix approach. Here, the image is obtained by solving a linear system of equations involving pre-measured data from a point sample moved over the later reconstrution grid. A study of these pre-measured data, or system matrices, is a useful way of gaining insight into the MNP properties. Furthermore, repetitive measurement and comparison of medium-sized system matrices is a convenient quality assurance (QA) approach for MPI scanners. Unfortunately, the size of the datasets, which easily reaches dozens of gigabytes, presents an obstacle for a visual inspection and analysis. Here we present a tool for convenient inspection of MPI system functions with versatile navigation and visualisation features.

I. Introduction

Since the introduction of MPI by Gleich and Weizenecker in 2005 [1] many advances have been made in the theoretical understanding of the imaging properties of MNP based tracer materials. Such understanding is essential for reliable reconstruction of imaging data. So far, two distinct reconstruction algorithms have been developed for MPI. Direct reconstruction from the time-dependent acquisition data, typically termed X-space reconstruction, has successfully been realized for MPI systems with mostly uniaxial fast field modulation that can be well described as linear shift-invariant (LSI systems) [2] . This class of systems includes current implementation of field-free-line scanners with slow line rotation. On the other hand, 3D MPI with high frame rates has only been practically demonstrated on systems with 3D encoding along lissajous trajectories. On these systems, the shift invariance is violated due to the complex interplay between the MNP dynamics and the encoding trajectory. Therefore, image reconstruction on such systems relies on pre-measured or precalculated system functions, where the particle response to the encoding fields is recorded or simulated for a delta sample moved sequentially to all positions of the planned reconstruction grid [3, 4]. To allow filtering and to improve reconstruction efficiency, the time-course signal is then transformed to the spectral domain. Spectra for all spatial positions are combined into a system matrix, which contains the spectrum for a single position in each column, and the spatial distribution of a single harmonic frequency in each row.

MPI system functions are acquired by a tedious calibration procedure, which requires many hours of stable scanner operation. Thus, any possible flaws of the scanner such as amplitude drifts, signal dropouts, spikes, position misalignments etc., will invariably show up in measured system function data, and their detailed inspection is a useful way of asserting reliable hardware

 © 2017 Infinite Science Publishing

operation. Systematic repetitive measurements of stable reference samples and statistical comparison of the results can be used as a routine quality assurance procedure. Furthermore, system functions are not only useful and necessary for image reconstruction, they are also a valuable source of information on the MNP properties, where the peculiar relaxation behaviour can manifest itself as phase differences between distinct spatial positions along the trajectory. Unfortunately, the analysis of system matrices is often rendered difficult by the sheer size of the datasets. For example, a system function based on data acquired on three channels with a detection bandwidth of 1.25 MHz and a frame rate of 46.42 Hz for a $32 \times 32 \times 32$ grid will result in a 42.3 GB data set containing the complex modulation amplitudes for each spatial position, channel and frequency bin. At many frequencies, the modulation depth is below the noise floor for all spatial positions. Hence there is need for a tool that allows quick navigation in the large datasets with the ability to selectively show significant signal components.

II. Theory

A 3D MPI scanner with Lissajous encoding employs different excitation frequencies on three drive field (DF) coils that produce mostly orthogonal fields which are superimposed to a static selection field (SF). To first order, the DF can be modelled as time-dependent homogeneous fields $H_{DF\{X,Y,Z\}}$, whereas the SF is modelled as a linear gradient field H_{SF} with its principal axis aligned with the system's z axis. Thus, the magnetic field at a spatial position $\{x, y, z\}$ is given by

$$\vec{H}(x,y,z,t) = \begin{pmatrix} -\frac{1}{2}G\,x + \hat{H}_{DFX}\sin\omega_x t \\ -\frac{1}{2}G\,y + \hat{H}_{DFY}\sin\omega_y t \\ G\,z + \hat{H}_{DFZ}\sin\omega_z t \end{pmatrix} \quad (1)$$

where G is the nominal selection field strength, $\hat{H}_{DFX}$, $\hat{H}_{DFY}$, and $\hat{H}_{DFZ}$ are the drive field amplitudes on each excitation channel, and ω_x, ω_y, and ω_z are the respective channel frequencies. The repetition rate of the lissajous pattern is given by the least common multiple (LCM) of the three frequencies. The field-free point (FFP) of the selection field traverses a volume given by the dimensions $4 \cdot \hat{H}_{DFX}/G \times 4 \cdot \hat{H}_{DFY}/G \times 2 \cdot \hat{H}_{DFZ}/G$, which is termed *Drive field Field Of View*, or V_{DF}.

The non-linear magnetization behaviour of the MNPs causes the generation of higher harmonics of the excitation frequencies as well as a wealth of intermodulation frequencies, where each frequency is determined by a triplet of integral multipliers $k_x, k_y, k_z \in \mathbb{Z}$:

$$\omega_{\{k_x,k_y,k_z\}} = k_x \cdot \omega_x + k_y \cdot \omega_y + k_z \omega_z \quad (2)$$

Note that $k_{\{x,y,z\}}$ can be negative, and that a given frequency may be expressible by different sets of mixing coefficients.

The mixing order κ is defined by

$$\kappa = |k_x| + |k_y| + |k_z| \quad (3)$$

and the harmonic band β by

$$\beta = k_x + k_y + k_z \quad (4)$$

Note that adjacent harmonic bands may overlap in frequency. Furthermore, frequencies that are expressible by different sets of mixing coefficients may also be assignable to multiple bands. Typically, absolute signal intensity decreases with increasing mixing order.

Each row of the system matrix contains the spatial distribution of a different frequency and channel. These matrix rows can be ranked according to their signal-to-noise ratio (SNR) $\sigma(\omega, i)$ after background correction, which is defined by

$$\sigma(\omega,i) = \frac{\frac{1}{V_{DF}}\int_{V_{DF}} \left|\tilde{u}(\omega,i,\vec{r}) - \overline{\tilde{u}_{BG}(\omega,i)}\right| dV}{|\mathrm{Var}(\tilde{u}_{BG}(\omega,i))|}. \quad (5)$$

Here V_{DF} is the volume covered by the FFP movement, ω is the specific frequency, i is the receive channel index, $\tilde{u}(\omega, i, \vec{r})$ is the modulation amplitude observed in channel i at the spatial position $\vec{r}$ at this frequency, and $\overline{\tilde{u}_{BG}(\omega,i)}$ is the average background signal obtained in channel i at frequency ω with the sample located outside the sensitive detection area. As noise model, the variance of said background signal is chosen which is remeasured frequently during system function acquisition.

For MNPs with infinitely fast relaxation, the magnetization change will follow the excitation signal without phase lag everywhere, so no spatial dependence of the signal phase is expected. Likewise, the signal phase should not vary with harmonic number. Deviations from this behaviour are a clue to dynamic particle properties and may be of particular interest during system function analysis [5].

A detailed analysis and derivation of the static MPI system function structure has been given by Rahmer et al. [6].

III. Viewing tool

In this section, **SFView**, a software tool for viewing and analyzing system matrices is presented, and its features, technical requirements, and implementation details are discussed.

III.I. File format support

SFView natively supports the file formats and directory layouts of the Bruker Preclinical MPI System [7, 8]. This system stores the actual system matrix, precomputed SNR tables, and reference background spectra in flat binary files, and the descriptory meta data in several plain

10.18416/ijmpi.2017.1706006
© 2017 Infinite Science Publishing

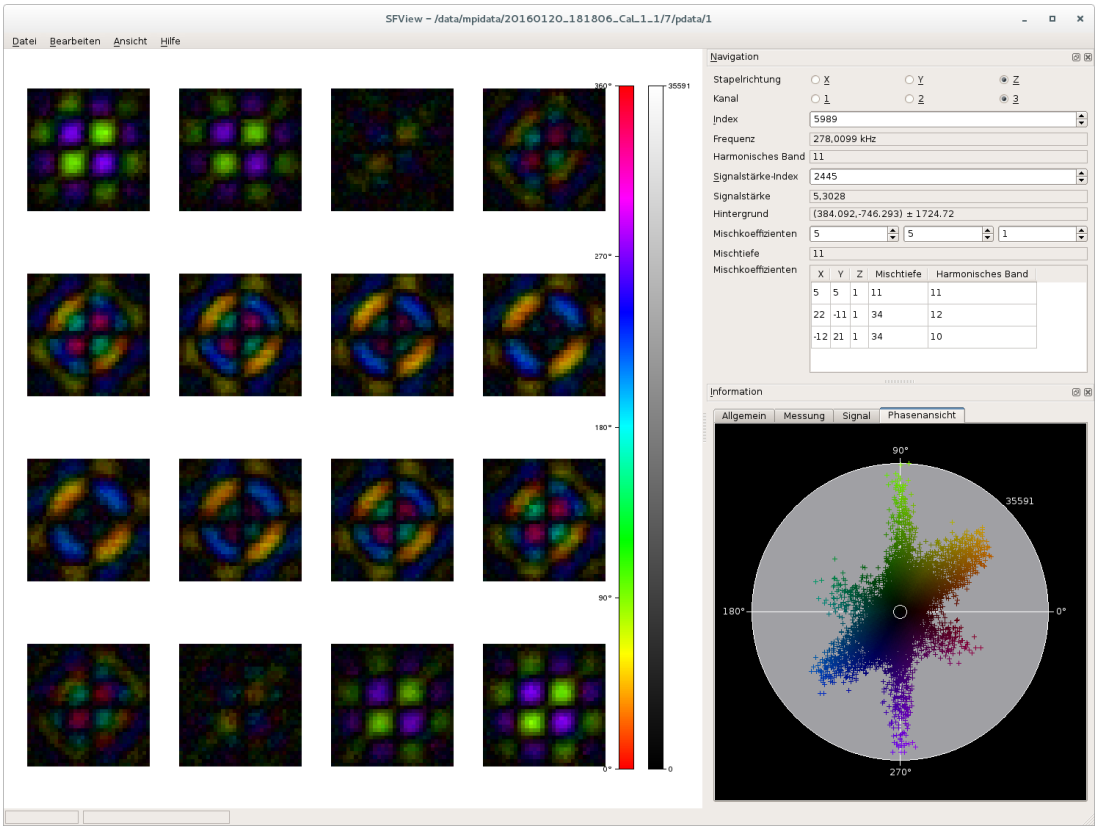

Figure 1: **SFView** showing the spatial distribution of signal intensity of diluted Resovist (100 mmol Fe/L) at a harmonic frequency of 279.0099 kHz in the scanner's Z channel using a complex-valued color map. Navigation and information panels are docked at the right side. The information panel shows a scatter plot of magnitude/phase values for the shown system function component. The white circle in this plot indicates the Z channel's background signal variance at this frequency.

text files based on the JCAMP-DX standard [9] using private tags with mnemonic names. From these meta data, the layout of the binary files can be inferred. The actual system function data are stored twice, with and without background correction.

Additional support for the recently proposed MDF file format [10] is in preparation.

III.II. Visualization options

Three different color maps are provided for system function visualization. A standard gray scale presentation of absolute intensities as used in [6] is available as well as a 'jet' scale similar to Matlab™ which permits a finer scale resolution. As an alternative, a complex mapping is provided which maps absolute intensity to color brightness and phase angle to hue (see Fig. 1). The three-dimensional signal distribution is presented in separate layers, the orientation of which can be changed using the navigation panel or via tool buttons. Individual layers can be zoomed to full screen.

III.III. Data navigation

The navigation panel of **SFView** (see Fig. 2) allows navigation by

- Receive channel
- Absolute frequency
- SNR rank, or
- Mixing coefficients.

Information about harmonic band, mixing order, SNR, and background signal intensity are provided as well as other possible combinations of mixing coefficients corresponding to the same frequency. Together, these navigation tools allow systematic investigation of the frequency mixing properties of the MNPs.

III.IV. Information panel

An information panel provides meta information about the dataset such as measurement parameters and SNR statistics. Such SNR statistics are useful for long-term stability and reliability assurance of MPI systems, as long as calibration samples with stable and reproducible performance are available.

10.18416/ijmpi.2017.1706006
© 2017 Infinite Science Publishing

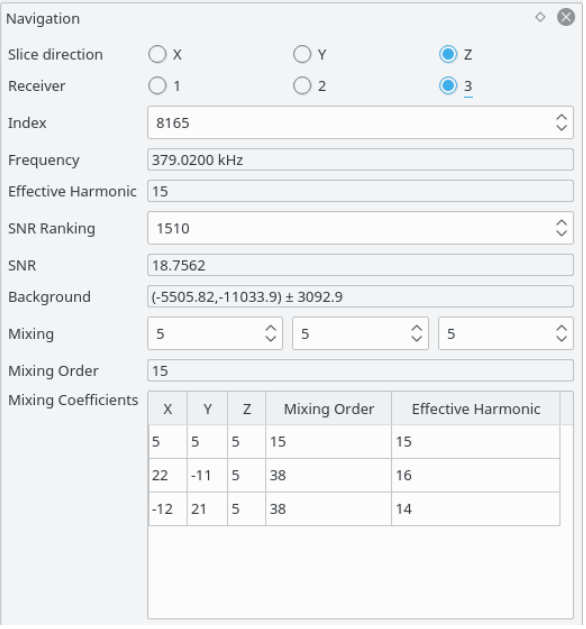

Figure 2: Navigation panel of **SFView**.

A particularly interesting function in this panel is an interactive phase/magnitude distribution plot that displays the distribution of the voxel values of the currently shown system matrix row in a complex plane. This feature is visible in the bottom right corner of Fig. 1. Hovering the mouse either in the matrix display or in the phase/magnitude distribution plot highlights the corresponding pixel in the other display to allow localization of particular features. A circle in the phase/magnitude distribution plot indicates the noise variance level $|\mathrm{Var}(\tilde{u}_{BG}(\omega, i))|$ of the background signal.

III.V. Example

As an example, Fig. 1 shows the distribution of magnitude/phase values for the harmonic frequency 278.0099 kHz, corresponding to mixing coefficients $k_x = 5$, $k_y = 5$, $k_z = 1$) in the Z channel of a Bruker Preclinical MPI System (Charité Berlin / PTB Berlin) for a diluted Resovist sample (100 mmol Fe/L). Three lobes are discernible in the phase plot. The dominant lobe ($90° \rightarrow 270°$) in green/purple color can be assigned to the top and bottom slices of the volume. A second lobe with a broader phase distribution roughtly in $45° \rightarrow 225°$ direction in orange/blue color arises from the outer area in the central planes, and a smaller lobe in the $-30° \rightarrow 150°$ direction shown in cyan/red colors originates from the center of the system function component. Interestingly, this third component is markedly reduced for samples with higher concentration (data not shown).

IV. Implementation

SFView is implemented in C++ using the Qt toolkit (version 5.6, or higher). Currently, there are no dependencies on external libraries or direct OS dependencies, ensuring high portability. **SFView** uses memory-mapped I/O of the data files to avoid the time and memory consuming process of loading the actual data files into computer memory in their entirety. This ensures fast opening of system function data and allows quick navigation even within large datasets while maintaining low memory requirements.

As an example, **SFView**'s memory usage increases by just 10 MB after opening the $32 \times 32 \times 32$ voxel / 1.25 MHz bandwidth / 3 channel system matrix mentioned in the introduction despite of the 42.3 GB used on disk. The increased memory usage after opening a system matrix is mostly due to lookup tables used for fast navigation. For the given system matrix, display of the spatial signal distribution at a single harmonic frequency on a given channel requires 0.5 MB to be mapped from disk into memory, which is accomplished in a few tens of milliseconds even for slower hard disks or network mounted storage. Thus, **SFView** performs well even on older hardware.

SFView is available with English and German user interface localization. It requires a 64-bit operating systems and has been successfully been tested on several Linux distributions as well as on Windows (versions 7 & 10). It is expected that **SFView** will be easily adaptable to other OS for which the Qt toolkit is available.

License **SFView** is provided under the General Public License V2 and can be obtained from `http://it.hs-pforzheim.de/personen/heinen/software/sfview.html` either in source form, as installable packages for CentOS or OpenSuse, or as a Windows installer binary.

V. Conclusion

SFView is a convenient and useful tool for manual inspection and analysis of large MPI system function data sets. It can be used for data quality inspection prior to image reconstructions as well as for scanner performance assessments. Powerful visualization options can provide additional insight into the spatial dependency of signal phase and amplitude as a route to an improved understanding of the complex particle dynamics during fast 3D-encoded MPI imaging.

References

[1] B. Gleich and J. Weizenecker. Tomographic imaging using the nonlinear response of magnetic particles. *Nature*, 435(7046):1214–

 © 2017 Infinite Science Publishing

1217, 2005. doi:10.1038/nature03808.

[2] P. W. Goodwill and S. M. Conolly. The x-Space Formulation of the Magnetic Particle Imaging process: One-Dimensional Signal, Resolution, Bandwidth, SNR, SAR, and Magnetostimulation. *IEEE Trans. Med. Imag.*, 29(11):1851–1859, 2010. doi:10.1109/TMI.2010.2052284.

[3] J. Weizenecker, B. Gleich, J. Rahmer, H. Dahnke, and J. Borgert. Three-dimensional real-time in vivo magnetic particle imaging. *Phys. Med. Biol.*, 54(5):L1–L10, 2009.

[4] T. Knopp, T. F. Sattel, S. Biederer, J. Rahmer, J. Weizenecker, B. Gleich, J. Borgert, and T. M. Buzug. Model-Based Reconstruction for Magnetic Particle Imaging. *IEEE Trans. Med. Imag.*, 29(1):12–18, 2009. doi:10.1109/TMI.2009.2021612.

[5] R. J. Deissler and M. A. Martens. Dependence of the Magnetization Response on the Driving Field Amplitude for Magnetic Particle Imaging and Spectroscopy. *IEEE Trans. Magn.*, 51(2):6500904, 2015. doi:10.1109/TMAG.2014.2322579.

[6] J. Rahmer, J. Weizenecker, B. Gleich, and J. Borgert. Signal encoding in magnetic particle imaging: properties of the system function. *BMC Medical Imaging*, 9(4), 2009. doi:10.1186/1471-2342-9-4.

[7] J. Franke, U. Heinen, A. Weber, N. Baxan, U. Molkentin, S. Hermann, W. Ruhm, and M. Heidenreich. Initial Results of the First Commercial Preclinical MPI Scanner. In *International Workshop of Magnetic Particle Imaging*, 2014.

[8] M. G. Kaul, O. Weber, U. Heinen, A. Reitmeier, T. Mummert, C. Jung, N. Raabe, T. Knopp, H. Ittrich, and G. Adam. Combined Preclinical Magnetic Particle Imaging and Magnetic Resonance Imaging: Initial Results in Mice. *Fortschr. Röntgenstr.*, 187(05): 347–352, 2015. doi:10.1055/s-0034-1399344.

[9] R. S. McDonald and P. A. Wilks Jr. JCAMP-DX: A Standard Form for Exchange of Infrared Spectra in Computer Readable Form. *Appl. Spectrosc.*, 42(1):151–162, 1988.

[10] T. Knopp, T. Viereck, G. Bringout, M. Ahlborg, J. Rahmer, and M. Hofmann. MDF: Magnetic Particle Imaging Data Format. *arXiv:1602.06072 [physics.med-ph]*, 2016.

 © 2017 Infinite Science Publishing